On the economic feasibility of tidal range power plants

Konstantinos Pappas, Nguyen Quang Chien, Ilias Zilakos, Lindsay Beevers, Athanasios Angeloudis

A non-peer reviewed preprint submitted to EarthArXiv, also submitted for consideration to the Royal Society Proceedings A.

On the economic feasibility of tidal range power plants

Konstantinos Pappas[a], Nguyen Quang Chien[a], Ilias Ziliakos[b], Lindsay Beevers[a], Athanasios Angeloudis[a,]

[a]*School of Engineering, Institute for Infrastructure and the Environment, University of Edinburgh, UK*
[b]*Tidetec, Oslo, Norway*

Abstract

The potential energy associated with tides presents a sustainable energy resource that remains largely untapped. Uncertainties on the economic case of tidal range power plants are a known obstacle. Research on tidal range structures suggests energy yield may be maximised through operation strategy optimisation and that impacts can be mitigated through design optimisation. While instructive, these perspectives alone are insufficient to support feasibility of individual projects. We integrate operation optimisation and hydrodynamic impact analyses within a cost evaluation framework for tidal range structures focusing on capital costs and levelised cost of energy (LCOE). Once benchmarked against 11 historic proposal cost projections, we perform a re-design of 18 tidal power plants to deliver a comprehensive comparative basis across a diverse range of sites in the UK. Tidal power plant operation is simulated in regional shallow water equation models, acknowledging tide variability. The cost evaluation framework demonstrates the impact of geospatial variations on key cost components and the re-design process indicates transformative implications in that equivalent and lower LCOE values can be achieved for designs at a substantially lower capital cost. Given how the latter hinder development, we show how tidal range schemes could be far more economically feasible than commonly perceived.

1. Introduction

Tidal range energy features predictability and partial flexibility that could contribute to meeting Net-Zero goals across several countries [1, 2, 3]. The underlying resource is the result of interactions between tidal wave propagation and the coastal geomorphology [4]. Specifically, tide resonance, shoaling and funneling effects along coastal embayments and estuaries can amplify tidal wave height, corresponding to substantial potential energy reserves. Depending on the magnitude, these can render the exploitation through tidal power plants feasible [5]. Tidal power plants of various sizes have operated in France [6, 7], Canada [8],

Email address: a.angeloudis@ed.ac.uk (Athanasios Angeloudis)

Russia [9], China [5] and, most recently, in South Korea [10]. The UK, despite its relatively small size, has an estimated potential energy converging to ∼12.6 % of the global available resource [11]. This amounts to a highly concentrated resource hotspot, and has been at the epicentre of industrial efforts to harness it given opportunities to complement an increasingly more diversified energy mix [12]. In the UK, several tidal range infrastructure proposals have been considered to-date with an estimate that ≈ 15% of the country's electricity needs could be sourced from this technology [13]. Large-scale options include variants of a Severn Barrage, such as the STPG (1987) and the Hafren Power (2012) schemes [14]; these were previously rejected on both economic and environmental viability grounds. More environmentally conservative options followed such as the Swansea Bay tidal lagoon project by Tidal Lagoon Power Ltd [15]. The lagoon concept was received favourably by the UK Government's independent "Hendry review" [16]. Even so, the UK Government eventually dismissed the pilot scheme at Swansea, questioning the project value relative to more mature technologies such as nuclear and offshore wind [17]. Thus, there is a research gap where further exploration into economic viability of schemes is needed in order to overcome existing barriers.

Despite obstacles faced by technology proponents on economic feasibility, research on the subject is scarce compared to other aspects such as environmental impact assessment [18, 19] and operation performance optimisation [20, 21]. The economic viability of renewable energy schemes typically concentrates on the quantification of levelised cost of energy (LCOE). LCOE is widely used to evaluate the cost and performance of energy conversion technologies [22], primarily due to its simplicity in combining capital (CAPEX) and operational (OPEX) costs. Within the broader tidal energy remit, LCOE studies concentrate on the upscaling of in-stream turbine arrays, which target the kinetic energy from high-velocity tidal currents [23, 24, 25]. On tidal range energy, few studies perform a formal breakdown of the capital and operation costs of different schemes. An early study by [26] focused on the Bay of Fundy, Canada, to inform the design of the Annapolis Royal power station. This was recently adapted for application to the UK [27, 28] for schemes in the UK's coast, with a similar approach documented by [29]. While valuable, varying assumptions are made within the calculation of influential components across studies. Deviations across methodologies, spatiotemporal differences, and simplifications that omit site-specific geospatial features inhibit the identification of opportunities to support the project economic case and drawing robust conclusions for the industry. In addition, sensitivities of LCOE to regional policies add to this uncertainty [30], while concepts of economies of scale and benefits of predictability are challenging to quantify in the absence of a more tailored framework to assess tidal range developments. Moving forward, a consistent calculation of its constituent components capital (CAPEX) and operational (OPEX) would be instructive and is needed to inform the next steps of this sustainable energy technology.

We seek to inform this design challenge in a manner that includes the geospatial sensitivity of different studies to costs, while demonstrating an approach to establish a robust comparative basis to assess different tidal range structures. In this process, we include steps to acknowledge tidal power plant hydrodynamic impacts [19] and embed an operational performance optimisation step [20]. This recognises how these steps have been oversimplified or excluded in economic analyses to-date which could introduce a tangible level of uncertainty. In demonstrating the implications of such a method, we consider the West coast of the UK. The region includes numerous case studies, with key examples summarised in Table 1. Many tidal power concepts have been contemplated to-date that vary in terms of location, design rationale, and scale. This region is unique as a known hotspot that is the focus of a significant number of idealised and practical case studies [5, 18, 14]. Capitalising on the diversity of these cases, there is an opportunity to provide new insights into the economic viability aspect. In parallel, we demonstrate the development of a method that is transferrable and scalable for the optimisation of future tidal power plants.

2. Methodology

We seek to determine the economic viability of tidal range power plants (i.e. lagoons and barrages) in a manner that is uniform across sites, scale and operation. This, sequentially, entails:

- the application of a regional shallow water equation model to accurately capture tide elevation and key constituents, as well as their interactions with the proposed tidal power plants over a representative lunar month.
- the integration of operational modelling as part of (a) hydrodynamic modelling (2-D) to assess tidal impacts and (b) as simplified (0-D) lumped-flow reservoir models within design optimisation (Sec. 2.2).
- the development of a LCOE calculation sequence (Sec. 2.3) combining geospatial data, hydrodynamic modelling outputs, and tidal power plant components.
- the methodological demonstration along the West of the UK coast, and the design of numerical experiments encompassing idealised and practical case studies as in Sec. 2.4.

2.1. Hydrodynamic modelling

In simulating the shelf's tide hydrodynamics, we solve the non-conservative form of the shallow water equations. We do so using *Thetis* [39], a 2-D/3-D model for coastal [40, 41] and estuarine [42] flows, implemented using the *Firedrake* finite element partial differential

equation solver [43]. *Thetis* was set up to include the following terms in the continuity and momentum equations

$$\frac{\partial \eta}{\partial t} + \nabla \cdot (H_d \mathbf{u}) = 0, \tag{1}$$

and

$$\frac{\partial \mathbf{u}}{\partial t} + \mathbf{u} \cdot \nabla \mathbf{u} - \nu \nabla^2 \mathbf{u} + f \mathbf{u}^{\perp} + g \nabla \eta = -\frac{\boldsymbol{\tau}_b}{\rho H_d}, \tag{2}$$

where $\mathbf{u}(u, v)$ is the depth-averaged velocity vector, η is the free surface elevation, $H_d = \eta + h$ is the total water depth (h is the mean water depth), $\boldsymbol{\tau}_b$ is the bed shear stress and $f = 2\Omega \sin(\zeta)$. On the latter, Ω is the angular velocity of Earth's rotation and ζ is the latitude. The third term in Eq. (2) is a viscous term representing diffusion and turbulence, whilst the fourth term represents the Coriolis force. The fifth term is the pressure gradient and the r.h.s. term is the bed shear stress contribution acting as a momentum sink. Considering that intertidal processes can greatly influence the tidal resource in coastal and estuarine zones, we applied the algorithm of [44] to include wetting and drying. The equations are discretised through a discontinuous Galerkin finite element approach and a piecewise linear ($\mathrm{P_{1DG}}$-$\mathrm{P_{1DG}}$) velocity-pressure finite element pair on an unstructured triangular mesh. For discretising irregular geophysical domains, we use the *qmesh* package [45]. A semi-implicit Crank-Nicolson timestepping approach is applied for integration in time with a constant timestep Δt.

Determinant to the model performance is the bed shear stress term, represented by the Manning's formulation as

$$\frac{\boldsymbol{\tau}_b}{\rho} = g n^2 \frac{|\mathbf{u}|\mathbf{u}}{H_d^{\frac{1}{3}}}, \tag{3}$$

where n is the Manning's coefficient ($\mathrm{m}^{-1/3}$ s); n is used as a calibration parameter for the hydrodynamic simulations against observed data. Calibration performance is measured by the following metrics: the root-mean-square error (RMSE), the normalised RMSE (NRMSE), the coefficient of determination (R^2), and the normalised standard deviation (σ_N), each expressed as

$$\mathrm{RMSE} = \sqrt{\frac{1}{N} \sum_i (X_i - G_i)^2}, \tag{4}$$

$$\mathrm{NRMSE} = \frac{\mathrm{RMSE}}{\sum_i (G_i - \overline{G})^2}, \tag{5}$$

$$R^2 = 1 - \frac{\sum_i (X_i - G_i)^2}{\sum_i (G_i - \overline{G})^2}, \tag{6}$$

$$\sigma_N = \frac{\sum_i (X_i - \overline{X})^2}{\sum_i (G_i - \overline{G})^2}, \tag{7}$$

respectively, where X is the simulated quantity (which could refer to time-varying series such as elevation or statistics at various locations, e.g. tidal amplitude or phase), while G is the corresponding gauged (measured) quantity.

2.2. Tidal power plant representation

Tidal power plants convert the potential energy from the tides into electricity using hydropower turbine principles [46]. Their operation and design are fundamentally linked to the resource and the localised basin characteristics.

2.2.1. Tidal range energy resource

The theoretical potential energy encompassed within a surface area A over a transition from peak to trough (or vice versa) for a tidal range R_i of a cycle i, assuming ideal conditions and neglecting energy losses (see [47]) can be expressed as follows:

$$E^i_{\max} = \frac{1}{2}\rho g A R_i^2 \tag{8}$$

where ρ is the fluid density, g is the gravitational acceleration. As the tide varies over long time scales (e.g. a nodal cycle spans 18.61 years), a comparative study that models tidal energy schemes over a short-term period (i.e. a lunar month of 29.53 days) must first establish a representative period. This is achieved using the custom rating method of [48]. This approach considers both the magnitude and variability of tides to extract a representative timeframe spanning a lunar monthly period.

2.2.2. Tidal power plant operational modelling & optimisation

Once tide conditions are predicted for a given timeframe, the operation of tidal power plants can be modelled either without (0-D) or with (in this case in 2-D) the consideration of direct hydrodynamic feedbacks [19]. Our 0-D modelling [20] requires the parameterisation of the hydraulic structures, and the impounded reservoir geometry. For hydraulic structures, turbines are represented through power curves (i.e. Hill Charts) as per [49, 11], based on low head bulb turbine designs. Sluice gates are represented through the orifice equation [11]. The reservoir geometry relies on the calculation of the impounded surface area with respect to the impounded water elevation, making use of geospatial data and an assumption of a constant water level in the impounded area. For consistency, the same hydraulic structure parameterisations are employed in 2-D modelling, while tidal elevations and basin geometry are directly modelled by *Thetis* thus capturing the water level variability. Tidal range impoundments are represented through a domain decomposition approach [15]. Both the 0-D

and the 2-D parameterisations are implemented as in [50] and the operational optimisation is defined based on the approach of [21].

2.2.3. Tidal power plant design

The modelling must follow design decisions on the hydraulic structure configuration, beginning with the size and specifications of the hydraulic structures. We build on the methodology used in [1] to determine a desired configuration based on the average potential energy. Accordingly, the predicted capacity is defined as

$$C = \eta_e \frac{\beta \rho g A \overline{R}^2}{T_{\mathrm{M}_2} C_F}, \tag{9}$$

where η_e is the expected generation efficiency, $\overline{R}$ is the mean tidal range, T_{M_2} is the M_2 tidal period, and C_F is a capacity factor. We introduce β as a factor relating the target operation strategy of the plant. If an ebb-only or flood-only strategy is expected then $\beta = \frac{1}{2}$; otherwise $\beta = 1.0$. We set $\eta_e = 0.40$ for an operation strategy without pumping. In turn, acknowledging economic feasibility constraints we choose $C_F = 0.20$, providing a break even target for the installed capacity. To ensure consistency across sites, design must adapt subject to the resource to maximise efficiency. The number of turbines and sluice gates is empirically defined as $N_t = C/P_{\max}$ and $N_s = N_t/2$, respectively. $P_{\max}$ is the turbine rated power, defined based on the available resource by setting the turbine rated head to $0.8 \times \overline{R}$ [2]. This modulation of rated head is introduced to ensure a fair comparison across sites tailoring the turbine Hill Chart parametrisation to the respective site.

2.3. Levelised cost of energy quantification

The LCOE is a standard metric for assessing the spread-out cost of energy and is widely used in power investments and policymaking [51]. In the context of nascent renewables, it is critical in gauging the level of subsidy required, and indicates the maturity of a technology relative to alternatives. The LCOE is defined here as [5]:

$$\mathrm{LCOE} = \frac{\mathrm{CAPEX} + \sum_{j=1}^{N} \frac{\mathrm{OPEX}}{(1+r)^j}}{\sum_{j=1}^{N} \frac{E_{yr}}{(1+r)^j}}, \tag{10}$$

where CAPEX is the total initial capital expenditure and OPEX is the operation and maintenance cost annually, E_{yr} is the annual energy generation, N is the expected lifecycle and r a interest rate or discount factor. For a typical tidal range structure of $N = 120$ years we assume a discount rate $r = 5\%$ [28]. Required input parameters in the LCOE calculation entail multiple assumptions, each containing some degree of uncertainty particularly when

drawing conclusions across technologies. The focus here is to apply this metric across studies based on the same timeframe and the same CAPEX and OPEX assumptions.

CAPEX costs can be broken down into individual mechanical and civil components (see Fig. 1), with the major cost contributors considered as the turbo-generators C_{t+g}, the powerhouse structure C_p, the sluice gates C_s, the embankment C_e, cofferdam C_c, major dredging operations C_d and the incorporation of shipping locks C_l where applicable. Therefore, we estimate the initial construction cost C_I as the aggregate of these individual cost elements as

$$C_I = \sum_{i=1}^{m} C_i \tag{11}$$

where m are the different cost components included. In this case, Table 2 provides the associated unit rates and equations for the key components identified. The definition of these costs requires inputs regarding mechanical and civil works. In order to capture distinct features across sites, the calculation relies heavily on geospatial data that covers bathymetry, and seabed type alongside the outlines of the tidal power plant schemes, as demonstrated by the expressions of Table 2. Sequentially, CAPEX must account for additional preliminary cost estimates and construction contingency as

$$\text{CAPEX} = C_I + C_{pr} + C_{cc}, \tag{12}$$

with the additional terms defined as in Table 3. Given the uncertainties with significant infrastructure projects and to enable comparisons with some reported data, an optimism bias is often incorporated C_b estimated as a percentage of the CAPEX costs.

Annual operation and maintenance costs (OPEX) account for the regular maintenance and oversight by a dedicated team of trained staff for turbines, sluice gates and other mechanical and civil components. There is a lack of up-to-date O&M data [29] given the limited number of operational tidal range projects. For consistency, annual O&M costs, including insurance and maintenance contracts, are assumed to be 1 % of the total capital investment [29], i.e.,

$$\text{OPEX} = 0.01 \times \text{CAPEX}. \tag{13}$$

Table 1: Examples and reported data on tidal range power case studies along the West Coast of the UK that form the catalogue of proposals to evaluate.

ID	Studies	Reported Capacity C (MW)	Turbines N_t	Turbines D (m)	Sluice Gates N_s	Sluice Gates A_s (m^2)	Impoundment Length L (km)	Operation Strategy	Reference
	Realistic case studies								
R1	Swansea Bay Lagoon (TLP)	320	16	7.35	8	100	9.6	Two-way & pumping	[11]
R2	Stepping Stones Lagoon (PB)	600	-*	-	-	-	10.6	Two-way	[31]
R3	Cardiff Bay Lagoon (TLP)	2010	67	8.90	16	150	20.8	Two-way	[32]
R4	Welsh Grounds Lagoon	1500	60	7.00	50	200	28.2	Ebb	[33, 34]
R5	Bridgwater Bay Lagoon	3600	144	-	25	-	16.1	Two-way	[33]
R6	West Somerset Lagoon (TEES)	2500	125	7.20	133	-	22.0	Two-way	[35, 36]
R7	Cardiff-Weston Barrage (STPG)	8640	216	9.00	166	210	16.1	Ebb	[11, 37, 32]
R8	Outer Severn Barrage	14800	370	-	320	144	20.0	Two-way	[29, 14]
R9	Colwyn Bay Lagoon (NWTE)	2500	125	8.00	40	150	32.0	Two-way	[35, 28]
R10	Mersey Barrage	700	28	8.00	18	144	1.8	Two-way	[35, 38]
R11	Morecambe Bay Barrage (NTPG)	3750	125	8.00	28	225	17.0	Two-way	[28]
	Idealised case studies								
I1	Swansea (SW)	1840	92	7.35	46	150	14.3		
I2	Cardiff (CA)	2200	110	7.35	55	150	12.9		
I3	Watchet (WA)	2220	111	7.35	55	150	12.8	Two-way	
I4	Colwyn (CO)	1940	97	7.35	48	150	11.9	with	[19]
I5	Liverpool (LI)	1400	70	7.35	35	150	14.9	pumping	
I6	Blackpool (BL)	1960	98	7.35	49	150	14.2		
I7	Solway (SO)	1820	91	7.35	45	150	12.4		

TLP: Tidal Lagoon Power Ltd, PB: Parsons Brinckerhoff Ltd, TEES: Tidal Engineering & Environmental Services Ltd, STPG: Severn Tidal Power Group, NWTE: North Wales Tidal Energy Ltd, NTPG: Northern Tidal Power Gateway

*Dashed entries indicate that exact specifications could not be found. These inputs were sequentially defined based on resource and design inputs as per Sec 2.

Table 2: Tidal power plant component cost modelling (Values adjusted in £ for 2016).

Component cost	Cost function	Definitions	Input Values	Comments
Turbine and generator cost	$C_{t+g} = N_t \times R_{t+g} \times H_R^{-0.5} \times P_{max}^{0.9} \times f$	N_t = Turbine number, R_{t+g} = Turbine and generator rate (£m$^{1.5}$/MWh), H_R = Turbine rated head (m), P_{max} = Rated power (MW), f = Scaling factor based on operational regime	$N_t = C/P_{max}$, $R_{t+g} = 3.36^*$ [27], $H_R = 0.8\overline{R}$ $f = \begin{cases} 1.125, & \text{for two-way operation} \\ 1. & \text{for ebb operation} \end{cases}$ [29, 27]	f is an estimated factor to enable bidirectional operation functionality.
Powerhouse cost	$C_p = N_t \times R_p \times 42\overline{R} \times D^2$	R_p = Powerhouse rate (£/m^3), $\overline{R}$ = Mean tidal range (m), D = Turbine diameter (m)	$R_p = 258^*$ [27]	
Sluice gate cost	$C_s = N_s \times R_g \times 18\overline{R} \times A_s$	R_s = Sluice gate rate (£/m^3), A_s = Sluice gate area (m^2)	$N_s = N_t/2$, $A_s = 150$ [19], $R_s = 290^*$ [27]	In the absence of input data on sluice gate specifications N_s is linked to the number of turbines N_t[3] and $A_s = 150$ m^2 is set as a default value [50].
Embankment cost	$C_e = R_e \times \sum_i \left(\int_0^{L_i} s_e H_e^2(x) + (W_e + 10 s_e) H_e(x) dx \right)$	R_e = Embankment rate (£/m^3), L_i = Embankment i^{th} segment length (m), H_e = Distance between seabed and crest level (m), W_e = Embankment crest width (m), s_e = Slope ratio	$R_e = 18^*$ [27] $W_e = 8$ (for a simple service road [27]) $s_e = \begin{cases} 2, & \text{for rock-filled gabions or geo-tubes used to face the slope} \\ 3, & \text{for hydraulic fill which has limited compaction} \end{cases}$ [27]	It is recommended at least $W_e = 25$ m for Access Category A and at least 16 m for Access Category B [29]
Cofferdam cost	$C_c = R_c \times \left[\sum_{i=1} (L_p^i + W_p^i + 20) \times 0.94 H_b^i + \sum_{j=1} (L_s^j + W_s^j + 20) \times 0.94 H_b^j \right]$	R_c = Cofferdam rate (£/m^3), L_p^i = Length (m), W_p^i = Width (m), H_b^i = Height of the high-tide depth + 3 m freeboard (m) of the i^{th} powerhouse. L_s^i = Length (m), W_s^i = Width (m), H_b^j = Height of the high-tide depth + 3 m freeboard (m) of the j^{th} sluice gates region	$R_c = 48^*$ [27]	We assume an allowance of 10 m on each of the hydraulic structures dimensions to facilitate the mobilisation of equipment.
Dredging cost	$C_d = \iint_{\mathbf{\Omega}} R_d(x,y) \left(H_p - H_a(x,y)\right) d\mathbf{\Omega}$	R_d = Dredging rate (£/m^3), H_p = Required powerhouse depth (m), H_a = Actual depth (m), $\mathbf{\Omega}$ = Total dredging area extends, i.e. $\mathbf{\Omega} = \bigcup_i \Omega^i \bigcup_j \Omega^j$, where $\Omega^i = [0, L_p^i] \times [0, W_p^i + 2l_a]$, $\mathbf{\Omega} = \bigcup_i \Omega^i \bigcup_j \Omega^j$, $\Omega^i = [0, L_s^i] \times [0, W_s^i + 2l_a]$, l_a = nominal flat bed allowance (m)	$H_p = 3 \times D + 3$ $l_a = 10$ [29] $R_d = \begin{cases} 106.4^*, & \text{for hard rock} \\ 70.53^*, & \text{for weathered rock/gravel} \\ 9.8^*, & \text{for soft material} \end{cases}$ [29] $W_p = \begin{cases} 10 \times D - 1, & \text{two-way operation} \\ 9.6 \times D - 8, & \text{ebb operation} \end{cases}$ [29]	A nominal flat bed allowance of 10 m is assumed on both the seaward and basin side of the turbine caisson [29]. We assume a depth requirement H_p for both the powerhouse and sluice gate sections.
Lock cost	$C_l = R_l \times (N_l \times V_l)^{0.76}$	R_l = Lock rate (£/m^3), V_l = Unit lock volume (m^3)	$R_l = 39670^*$ [29] $N_l = \begin{cases} 1, & \text{for lagoons or barrages with} < 5000 \text{ annual vessel movements (avm)} \\ 2, & 5000 \leq \text{avm} < 12000 \\ 3, & \text{avm} \geq 12000 \end{cases}$ [29] $V_l = \begin{cases} 15400, & \text{for small barrages and lagoons} \\ 384000, & \text{for large barrages or busy navigation routes} \end{cases}$ [29]	A single lock for maintenance activities is recommended [29]. Lock costs become significant in the case of barrages that are obstructing significant shipping routes.

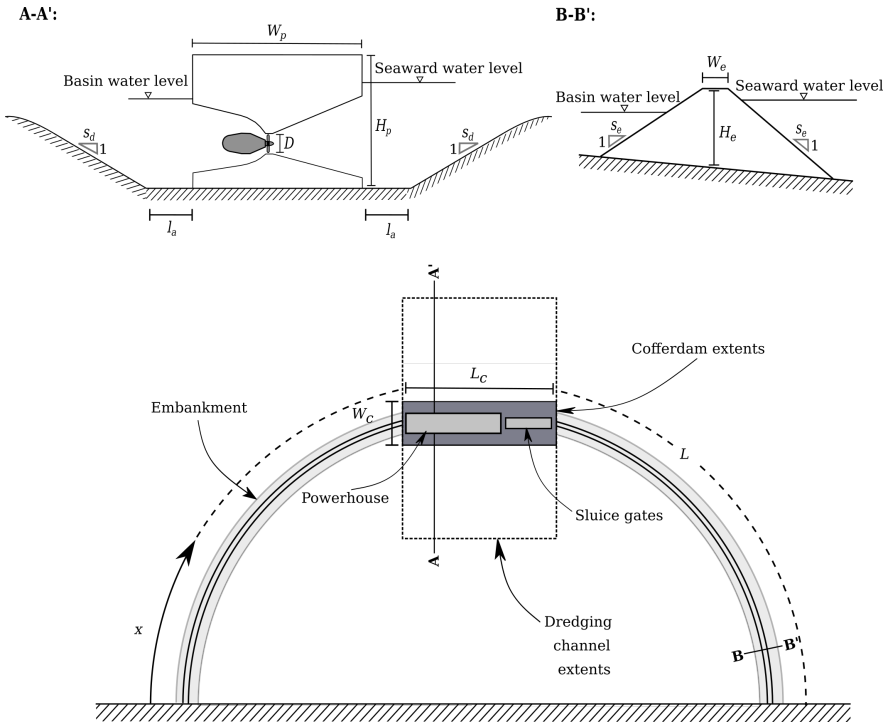

Figure 1: Definition sketch of an idealised tidal range lagoon, highlighting the key components that will contribute to the calculation of the initial construction investment C_I

2.4. Research approach

The West coast of the UK is selected to demonstrate our methodology as it hosts sites for both idealised and practical case studies (Table 1). The impoundment outlines are indicated in Fig. 2. There are two clusters of projects geographically. R1-8 and I1-3 are in the south within the Bristol Channel and the Severn Estuary, while R9-11 and I4-7 sit along the North Welsh and English coastline of the Irish Sea. The distribution of projects follows the available tidal range energy density which amplifies up to the mouth of the river Severn and similarly along the estuaries and bays of the Irish Sea. This amplification is primarily due to convergence to quarter wavelength resonance for the principal lunar and solar tide constituents M_2 and S_2 [53]. The resonance is further compounded to a lesser extent by shoaling of the tide and funnelling effects due to the shape of the coastline.

In capturing the tidal resource, we configure hydrodynamics models for the area. We adopt the computational domain extents of [19], established based on a sensitivity study on the Open Boundary Problem [54] once the idealised schemes I1-7 were introduced. The model bathymetry comprises two datasets which are brought to the same Mean Water Level (MWL) datum for consistency. Where available, 1 arc-second resolution data by Digimap[1]is

[1]Digimap. 2023 Marine Digimap. Edina Digital Service. See https://digimap.edina.ac.uk/ (accessed on

Table 3: Summary of costs that are proportional to CAPEX or the cost of main components.

Component	Cost function	Definitions	Input Values	Comments
Preliminaries cost	$C_{pr} = p \times (C_I - N_t \times C_{t+g})$ *	p = percentage of civil works cost (%)	p = 0.225 [29, 27]	Preliminaries refer to the costs associated with the preparatory work required before the construction phase. [29] assumes $p \sim 15$ % while [27], 30 %. We take the average of these two values as indicative input.
Construction contingency	$C_{cc} = q \times C_I$	q = percentage associated with the initial cosntruction cost C_I (%)	$q = 0.20$ [29]	Construction contingency is a budgeted amount of funds set aside to cover unforeseen events that might occur during the project construction phase.
Optimism bias	$C_b = \alpha \times$ CAPEX	α = Optimism bias percentage that is associated with CAPEX (%)	$\alpha = 0.45$ [52]	Optimism bias is a cognitive bias related to human tendencies in estimating project duration and costs. It is mostly anticipated as a fixed percentage to all potential schemes [29]. On the feasibility of tidal schemes in the Severn, a value 45 % of the CAPEX was assumed [52].

* $C_I - N_t \times C_{t+g}$ referred as civil works cost.

used, while the remainder is filled by 15 arc-second GEBCO[2] data. The model is forced at the seaward open boundaries at the continental shelf using eight constituents (M_2, S_2, N_2, K_2, O_1, Q_1, P_1, K_1) from the TPXO09[3] database, which are used to reconstruct pressure signals using *uptide*[4]. The major rivers are included through average flow based on the UK's National River Flow Archive. A representative tidal period over a lunar month starting from 20/10/2002 is selected as per Sec. 2(b)- 2.2.1. On mesh generation, a balance between computational efficiency and accuracy is sought, with different levels of resolution along coastlines, island features, and locations where tide gauges or tidal power plant schemes are located. Indicatively, the mesh for the ambient case (excluding tidal range structures) simulations consists of $\sim$ 60000 elements with a range of 150 - 15000 m in element side length. For validation, the tide gauge data provided by the British Oceanographic Data Centre (BODC[5]), with the calibration ensuring that tidal dynamics are represented adequately for an even comparison across schemes. All simulations use a $\Delta t = 100$ s.

On the levelised cost of energy calculations, the workflow of Fig. 3 is followed either in

10 August 2023)

[2]GEBCO. 2023 Gridded Bathymetry Data. See https://www.gebco.net/ (accessed on 10 August 2023)

[3]TPXO. Global Tidal Models. See https://www.tpxo.net/ (accessed on 10 August 2023)

[4]Kramer S. 2020 Uptide. See https://github.com/stephankramer/uptide (accessed on 19 December 2022)

[5]BODC. 2020 UK Tide Gauge Network. British Oceanographic Data Centre (BODC). See https://www.bodc.ac.uk/ (accessed 10 September 2023)

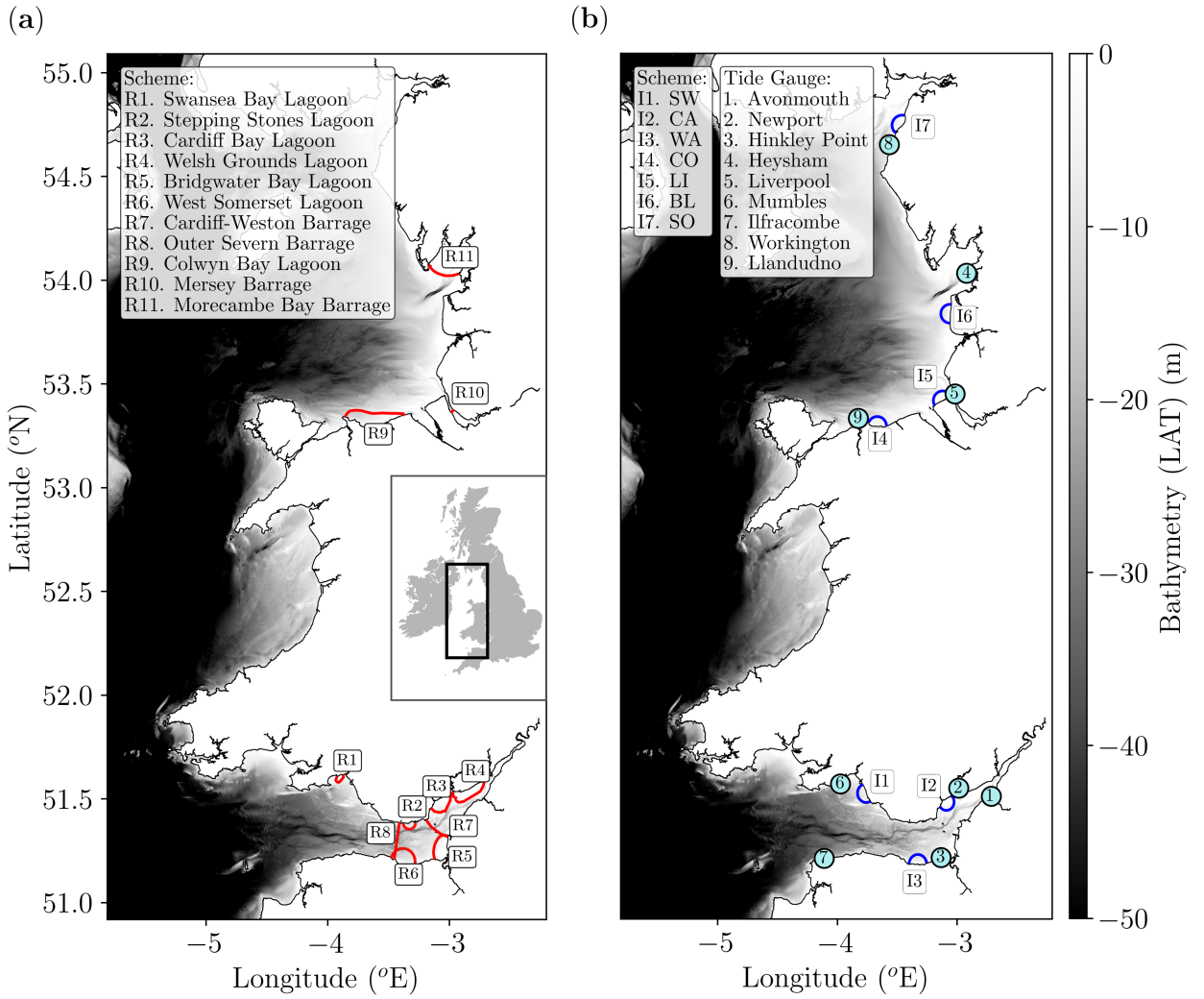

Figure 2: Map of potential/studied tidal range structures in the UK. Bathymetry (m) in 1 arc-second resolution from the Digimap[1] dataset. (a) Realistic schemes as per Table 1, (b) Idealised schemes [19] and tide gauge validation points utilised for the analysis.

full or partially (depending on design information availability), utilising bathymetric data (Step 1) from the Digimap[1] database, and seabed data from the British Geological Survey (BGS[6]). In cases where exact coordinates for hydraulic structures have been undefined (Step 2, Fig. 3), the deeper sections of the impoundment are preferred to satisfy depth requirements of hydraulic structures (that often demand a depth $h > 25$ m to minimise dredging overheads). To secure tide signals for each individual scheme (Step 3, Fig. 3), hydrodynamic models are constructed that include the tidal power plant impoundments. For practical cases (R1-12, Table 1)) this is done individually, while for idealised cases (I1-7,

[6]BGS. British Geological Survey. See https://www.bgs.ac.uk/ (accessed 15 July 2023)

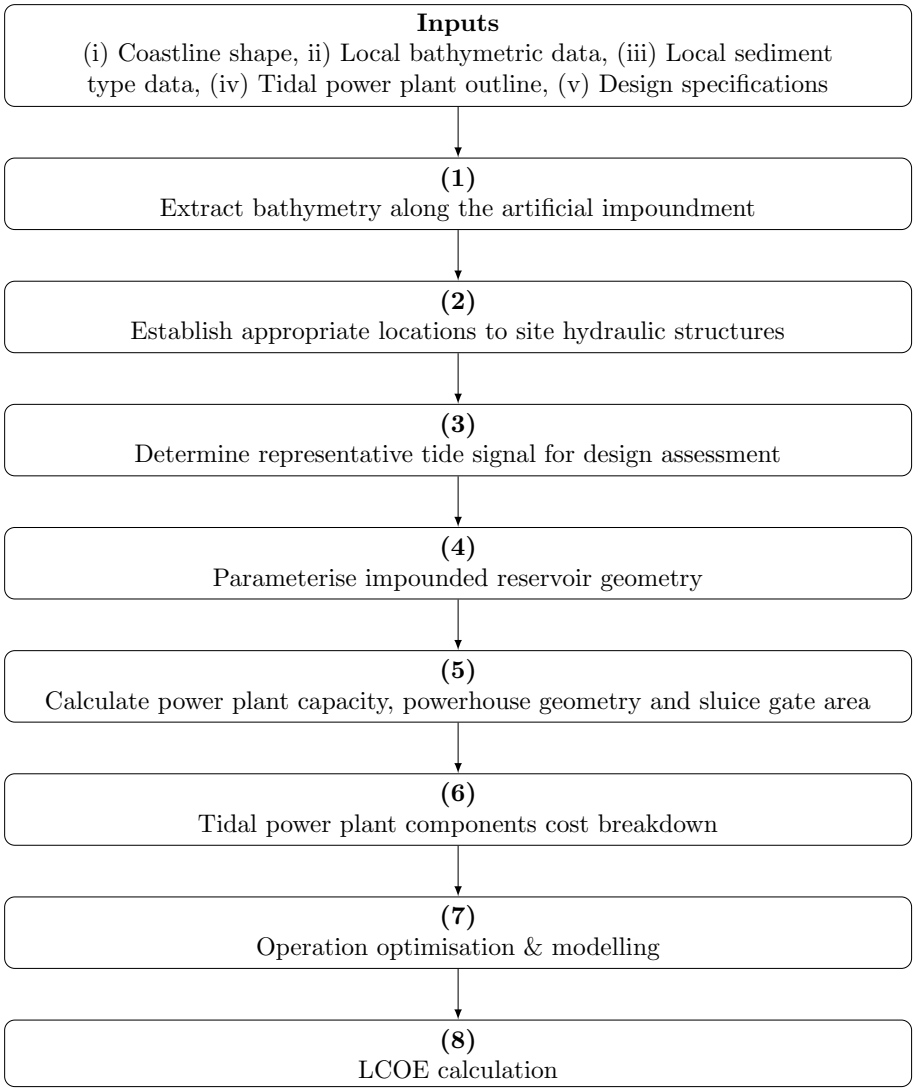

Figure 3: LCOE calculation workflow for a generalised tidal power plant design.

Table 1) this is done collectively as per [50]. An initial run of the hydrodynamics models without an explicit operation is conducted, to discern impacts on key tide constituents, and derive modified tide signals for the ensuing analysis. In turn, the reservoir bathymetry is parameterised to link the tidal power plant internal surface elevation with the storage volume due to intertidal regions along the coast (Step 4, Fig. 3). The resource available within the local tide signal, the reservoir geometry, and the design specifications of Sec. 2.2 combine to calculate the key plant components (Step 5, Fig. 3). This allows the quantification of the capital cost breakdown (Step 6, Fig. 3). In parallel, operation is optimised and modelled in 0-D as in Sec. 2.2, and then simulated in *Thetis* to observe any additional operation-related performance and hydrodynamic impacts (Step 7, Fig. 3). Annual Energy Projections (AEP)

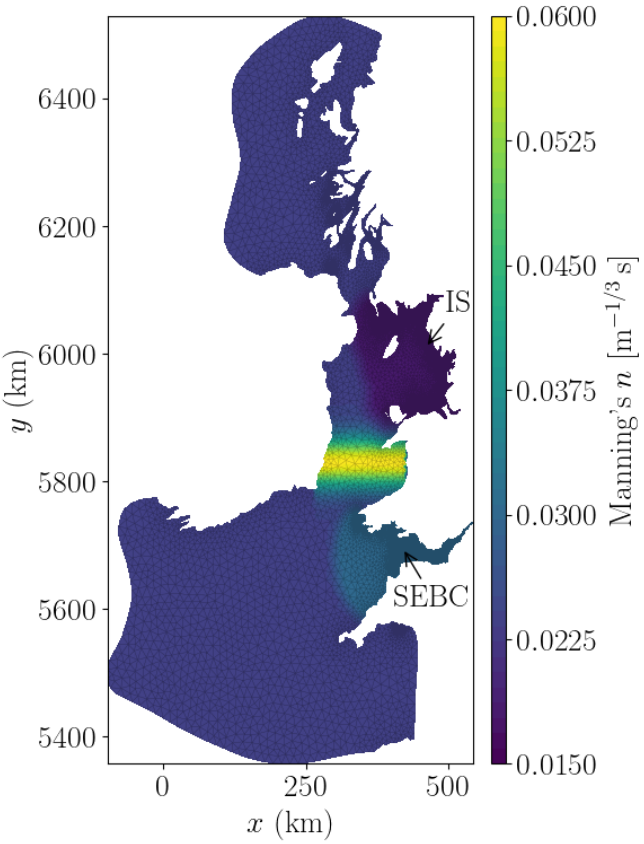

Figure 4: Computational domain, baseline mesh and Manning's n field for Scenario n_3. Coordinates are shown based on the UTM30N projection used within the *Thetis* hydrodynamic modelling. The areas of interest at the Severn Estuary and the Bristol Channel (SEBC) and the Irish Sea (IS) are also indicated.

are then combined with capital and operational costs to determine the LCOE of each case study (Step 8, Fig. 3).

This framework is first applied on the benchmarking against historic cost predictions for previous schemes. In turn, we consider the idealised schemes of [19] which were originally designed relying solely on operation optimisation. This is meant to demonstrate the value of the economic cost breakdown in evaluating different schemes. Finally, all schemes of Table 1 are redesigned based on an equal basis to deliver an objective comparison.

3. Results

3.1. Regional tidal hydrodynamics

3.1.1. Ambient resource modelling

Tidal hydrodynamics simulations use the computational domain of Fig. 4 as a baseline model. Unlike studies that focus on a single site [34, 55, 56], simulations here must ad-

equately capture the resource distribution across multiple areas where projects have been considered. Previous work [19] featured the same domain and imposed a uniform $n = 0.026$ $\mathrm{m}^{-1/3}$ s. This value leads to the tidal range being underestimated in the Severn Estuary and slightly overestimated in the Irish Sea (Fig. 5c), indicating a potential bias in the results when comparing designs between these areas. To examine the sensitivity to Manning's n, we considered both uniform and spatially-varying seabed friction fields. We present calibration results from three resistance fields (n_1, n_2, n_3) tested. The simplest approach was to use a single value for the whole domain, namely $n_1 = 0.026$ $\mathrm{m}^{-1/3}$ s as in [19]. Next, localised calibration at a region far from the immediate sites of interest within the Irish Sea was exercised. We superimposed on the n_1 field a Gaussian ridge with a peak of $n_{\max} = 0.06$ $\mathrm{m}^{-1/3}$ s and a standard deviation of $\sigma = 27$ km (Fig. 4). Located within the Cardigan Bay, this ridge serves to regulate the tidal flux between the Irish Sea and the Bristol Channel and the open seaward boundaries; the latter were weakly forced by harmonically reconstructed tidal signals. Finally, n_3 combines n_2 with a background uniform value of 0.024 $\mathrm{m}^{-1/3}$ s. The resistance is locally scaled at the SEBC ($\times 1.25$) and the IS coast ($\times 0.75$) to correct for opposing trends in tidal range witnessed in these regions as experienced in the uniform n_1 approach.

Among the 24 gauges listed by BODC[5], five are selected along the SEBC and four along the IS coast that have a minimum annual energy content of 94 $\mathrm{kWh/m^2}$ [48] and are close to the tidal power plant scenarios tested. The overall performance on tide constituents can be observed in Fig. 5a,b. Using a uniform Manning n_1 results in an RMSE = 0.095 m and $R^2 = 0.993$ for the principal lunar $\mathrm{M_2}$ tide constituent. Through n_2, the $\mathrm{M_2}$ amplitude deviations increase (RMSE = 0.099 m, $R^2 = 0.992$) while for the principal solar constituent ($\mathrm{S_2}$) deviations reduce. In n_3, the overall RMSE of 0.092 m for the $\mathrm{M_2}$ is an improvement at the expense of the $\mathrm{S_2}$ amplitude and phase. The value of the calibration for this study can be assessed when observing the bias in Fig. 5c on the potential energy, which is the quantity targeted by tidal range energy systems. We see that the calibration actions successively improve the model's capacity to capture the energy at key tide gauges. This is also reflected in Fig. 6, showing for n_3 an improvement on the normalised standard deviation σ_N, which suggests that the model convincingly captures the elevation variations across sites of interest. On that basis, n_3 is chosen as the preferred resistance field used across all subsequent simulations that include tidal range systems.

3.1.2. Tidal power plant hydrodynamic impact

The introduction of hard infrastructure in macrotidal waters is expected to alter tidal dynamics [57, 19] and by extension the distribution of tidal energy fluxes across the continental shelf. The total impact of a scheme is a combination of both the presence of the structure and its specific operation [32]. Studies show that the far-field impacts that relate to the large

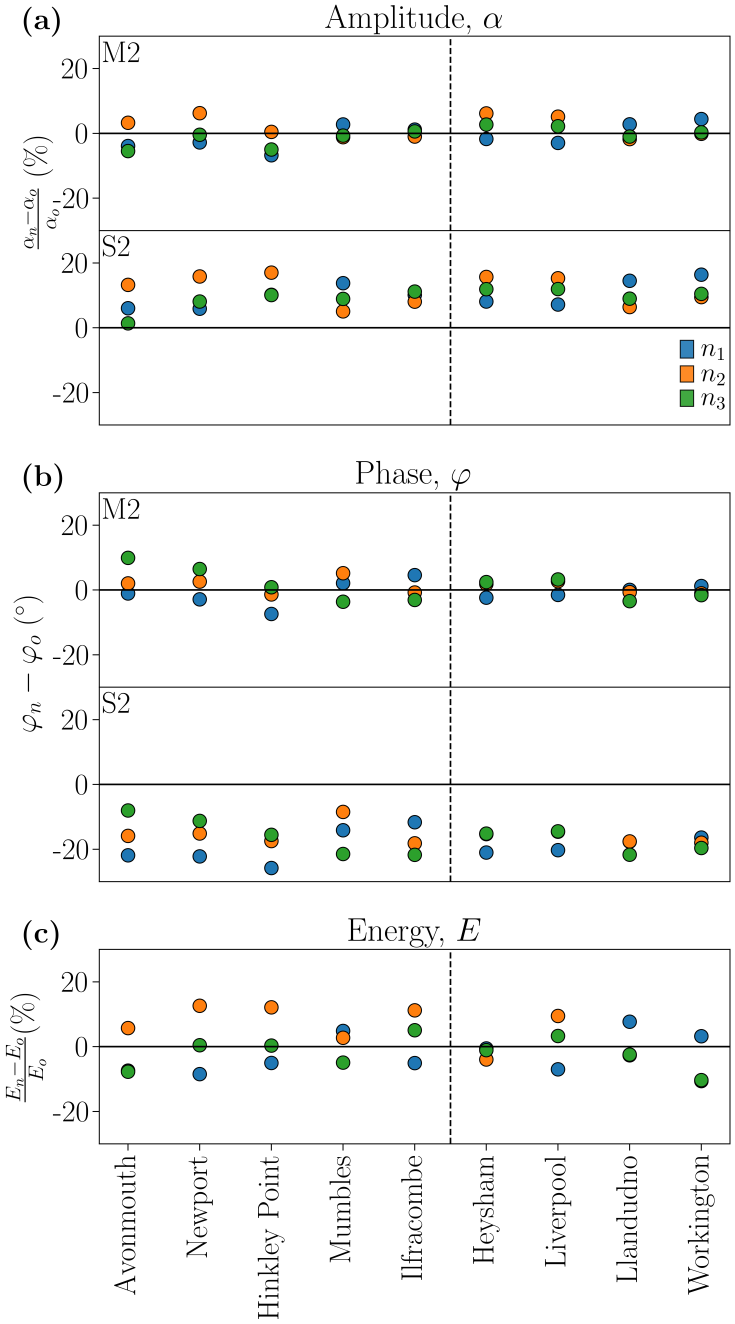

Figure 5: Biases in the predicted (a) amplitude α (m) and (b) phase ϕ (deg) for the principal tide constituents (M_2 and S_2), as well as predicted (c) theoretical monthly energy $E = \sum_{i=1}^{58} E^i_{max}$ (E^i_{max} as defined in Eq. 8) for the key gauges based on the tide gauge and predicted elevation data. The vertical black dashed lines separate on the left gauges in the Severn Estuary & Bristol Channel (SEBC) and on the right gauges in the Irish Sea (IS). Subscripts n and o denote the modelled and observed values respectively.

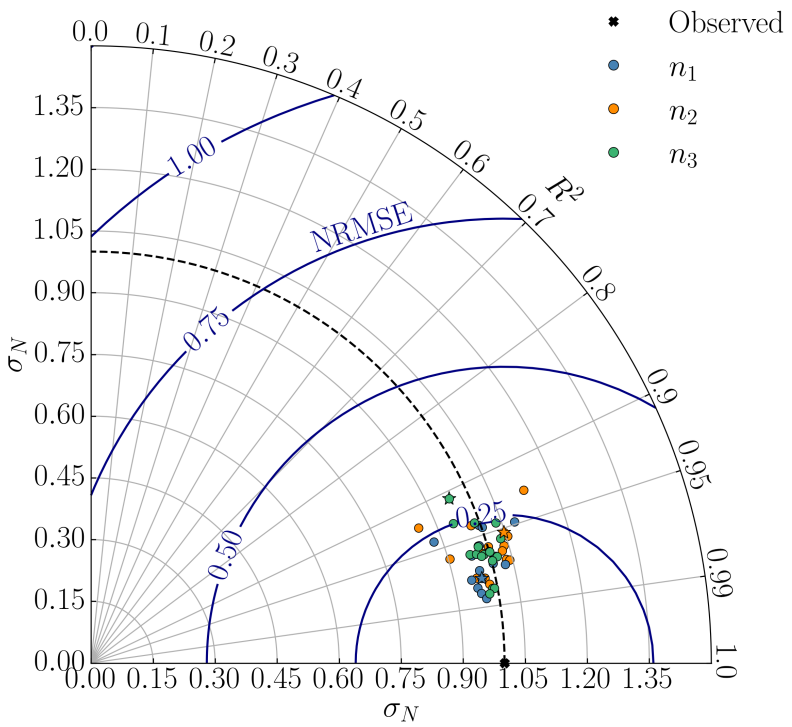

Figure 6: Taylor diagrams demonstrating the simulation performance for tide elevation predictions against 15-min gauged data over the same lunar months in terms of R^2, NRMSE and σ_N. The stars on the diagram represent metric values at Avonmouth, i.e. the gauge with the highest potential energy content.

scale tidal resource are a result of the impoundment as it alters basin geometry characteristics that lead to amplification of the tidal range [34]. The operation is expected to have a more localised influence at seaward hydrodynamics around the hydraulic structures. However, the operation dominates conditions within the impounded area. Table 4 summarises alternations in tidal range and associated energy to the ambient model (n_3) induced by the introduction of tidal energy schemes. Specifically, these values are sampled at the seaward side of turbine structures, for the operation optimisation. When examining individual designs, (R1-R11) a systematic reduction in tidal resource becomes evident. As anticipated for barrages that occupy the entire basin width, most substantial discrepancies are observed in the presence of the Cardiff-Weston (R7), the Outer (R8), and Mersey (R10) barrages with an impact to the potential energy content of –11%, –26%, and –14% respectively. Furthermore, the cumulative effects of I1-I7, result in a decrease of tidal energy resource of about 2-3% in Severn Estuary sites and an increase of 1-2% in the Irish Sea. This is in alignment with observations of [19] and shows a shift of some of the tidal energy flux from the SEBC to the IS resonant system.

Table 4: Impact of tidal range structures on annual mean tidal range $\overline{R}$ and theoretical energy density E. Initial determination of $\overline{R}$ and E are made during the specified representative tide month [48], followed by extrapolation to annual values. The subscript M denotes the modified tidal range and the associated potential energy density respectively at the seaward side of the hydraulic structure location.

ID	Studies	Tidal Range			Potential Energy Density		
		$\overline{R}$ (m)	$\overline{R}_M$ (m)	$\frac{\Delta\overline{R}}{\overline{R}}$ (%)	E (kWh/m^2)	E_M (kWh/m^2)	$\frac{\Delta E}{E}$ (%)
	Realistic case studies						
R1	Swansea Bay Lagoon	6.62	6.51	-2	90	88	-3
R2	Stepping Stones Lagoon	7.83	7.66	-2	126	120	-5
R3	Cardiff Bay Lagoon	8.64	8.47	-2	153	148	-3
R4	Welsh Grounds Lagoon	9.00	8.97	0	166	166	0
R5	Bridgwater Bay Lagoon	8.53	8.44	-1	149	146	-2
R6	West Somerset Lagoon	7.99	7.82	-2	131	125	-4
R7	Cardiff Weston Barrage	8.46	7.85	-7	147	130	-11
R8	Outer Severn Barrage	7.72	6.53	-15	122	90	-26
R9	Colwyn Bay Lagoon	5.50	5.42	-1	61	59	-3
R10	Mersey Barrage	6.77	6.25	-8	92	79	-14
R11	Morecambe Bay Barrage	6.36	6.27	-1	81	79	-3
	Idealised case studies						
I1	Swansea (SW)	6.69	6.59	-2	92	90	-3
I2	Cardiff (CA)	8.80	8.66	-2	159	154	-3
I3	Watchet (WA)	8.03	7.91	-1	132	129	-2
I4	Colwyn (CO)	5.62	5.63	0	63	64	1
I5	Liverpool (LI)	6.10	6.11	0	75	75	1
I6	Blackpool (BL)	6.00	6.04	1	73	73	1
I7	Solway (SO)	5.62	5.66	1	63	64	2

3.2. Tidal power plant cost assessment

3.2.1. Benchmarking of tidal power plant costs

The economic feasibility of tidal power plants is a challenging task to address, with several studies reporting CAPEX estimates and projections for individual schemes that are wide ranging. Table 5 reports on the costs associated with the realistic schemes (R1-R11) investigated in our study. For consistency, we first project all costs to the values of a reference year, in this case, 2016. Using the historic specifications of R1-R11 in Table 1, we optimised the operation for the original operation strategy, and calculate cost predictions in the form of CAPEX and LCOE. For the majority of the cases, the cost model provides estimates close to the published values which ranges between –24% and 30%. A significant deviation of 129% and –43% is observed for R5 where two values of 3.3 and 13.3 billion pounds (2016 price) were reported, which we consider an outlier that refers to different concepts for that area that share the same name. Reports on LCOE values for existing schemes are scarce, apart

Table 5: Benchmarking between reported tidal range schemes costs and calculated results based on the cost evaluation framework of Section 2.3 using a discount rate $r = 5\%$.

ID	Studies	Reported CAPEX Year	Reported CAPEX ($£_{year}$ bn)	Projected CAPEX ($£_{2016}$ bn)	Predicted CAPEX ($£_{2016}$ bn)	Percentage Difference (%)	E_{yr} (TWh)	Predicted LCOE (£/MWh)
R1	Swansea Bay Lagoon	2016	0.85 [58]	0.85	0.99	16	0.53	113
		2016	1.30 [59]	1.30		–24		
R2	Stepping Stones Lagoon	2012	1.70 [31]	1.84	2.39	30	1.14	126
R3	Cardiff Bay Lagoon	2016	8.00 [60]	8.00	4.94	–38	3.82	78
R4	Welsh Grounds Lagoon	2008	3.10 [61]	3.41	4.09	20	2.87	86
		2008	6.80 (10.10*) [33]	7.48		–45		
R5	Bridgwater Bay Lagoon	2008	3.00 [61]	3.30	7.57	129	4.12	111
		2008	12.00 (17.70*) [33]	13.20		–43		
R6	West Somerset Lagoon	2019	8.50 [62]	7.71	8.08	5	5.29	91
R7	Cardiff-Weston Barrage	2008	18.00 [61]	19.80	20.73	5	12.48	100
		2008	23.20 (34.30*) [33]	25.52		–19		
		2010	19.60 - 22.20 [14]	21.56 - 24.42		–4, –15		
R8	Outer Severn Barrage	2008	28.7 [61]	31.57	30.75	–3	16.15	115
		2010	31.00 - 34.70 [14]	34.72 - 38.86		–11, –21		
R9	Colwyn Bay Lagoon	2020	7.00 [28]	6.30	6.47	3	4.03	97
R10	Mersey Barrage	2011	3.50 [63]	3.85	3.97**	3	1.24	192
		2022	6.00 [64]	4.50		–12		
R11	Morecambe Bay Barrage	2019	7.96 [28]	7.20	7.62	6	3.65	126

* Optimism bias included. ** Three shipping locks have been taken into account.

from the Swansea Bay Lagoon scheme (R1) with a value quoted at 92.50 $£_{2012}$/MWh [21, 16] that translates to 99 $£_{2016}$/MWh. Our predicted value of 113 $£_{2016}$/MWh is within 15% of that range with the prediction difference attributed to our higher discount rate estimate of 5%.

3.2.2. Breakdown of tidal power plant costs

An enquiry follows on the breakdown of CAPEX to individual cost components and their sensitivity. This is the focus of Fig. 7. [19] delivered a framework that consistently optimises and assesses tidal lagoons (I1-I7) of the same size, with the design objective balancing energy yield and capacity factor. Their study emphasised energy yield, and excluded any form of costing. The costing framework shows CAPEX would vary between £3 - £6 Billions and an LCOE ranging at 150±25£/MWh for schemes occupying $\approx$ 40 km^2 of coastal space. Considering that the primary cost is associated with the turbines (which also correlates with many of the other components) we test a re-configuration of the arrangement based on a target $C_F = 0.2$ which is almost 2$\times$ the C_F of [50]. In Fig. 7 the CAPEX experiences decreases spanning from –49% to –60% while E_{yr} from –21% to –39%. Collectively, the redesign also corresponds to a remarkable reduction of LCOE, which exhibits a substantial

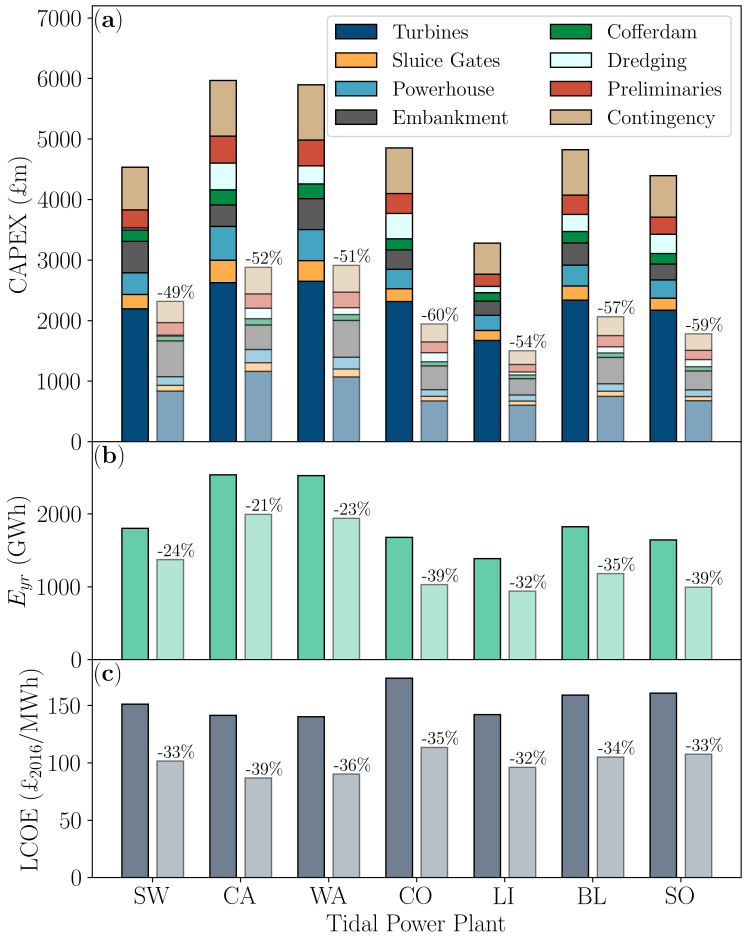

Figure 7: Cost and performance comparison of idealised tidal power plants in different locations (2016 prices). The initial designs [19] are represented by solid colours, while the adjacent semi-transparent bars indicate associated revised schemes. The figure shows (a) the breakdown of capital costs for various components of the power plants, (b) the predicted annual energy output for each location and (c) the levelized cost of energy (LCOE). The LCOE values were calculated using an interest rate $r = 5\%$ and a lifetime $N = 120$ years.

drop ranging from –32% to –39% bringing it to 100 ±15 £/MWh.

3.2.3. Evaluation of costing framework across case studies

The revised design of tidal power plant configurations based on a capacity factor $C_F = 0.2$ is then considered to provide a consistent design objective across all cases. Results for both idealised (I1-7) and realistic (R1-11) cases are summarised in Table 6. For CAPEX, a reduction is notable in the majority of the modified schemes, ranging from –5% in R9 to –46% in R5. Conversely, R4a, R7a, and R8 show an average CAPEX increase of ≈ +23%. On energy production, the net increase of C_F relative to original designs corresponds to a reduction in turbine numbers which naturally leads to a reduction in energy yield from –14% in R5 to –28% in R1. This is not always the case as R10 and R11 energy yield increases by

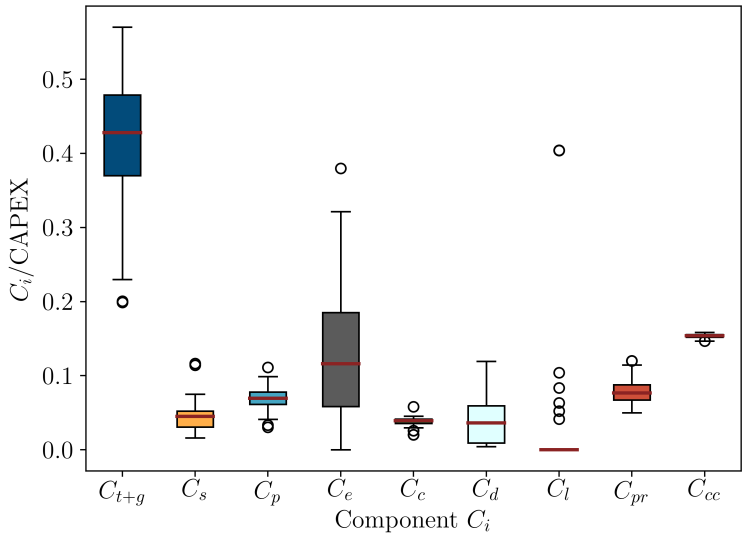

Figure 8: Box plot on the distribution of cost components across tidal range schemes examined in this study. The y-axis is the ratio of individual cost components (C_i) relative to the total capital cost (CAPEX) for that project. Cost components include turbo-generators C_{t+g}, sluice gates C_s, powerhouse C_p, embankment C_e, cofferdam C_c, dredging C_d, locks C_l, preliminaries C_{pr} and construction contingency C_{cc}. More details on the calculation of these quantities are provided in Table 2.

2% and 7%, respectively.

Applying the same cost component breakdown as in Fig. 7 we can understand how influential certain components can be on overall cost. Normalised by CAPEX, these costs are summarised in the plot of Fig. 8. We see the main cost drivers as the turbo-generators C_{t+g} with a mean value of 43%, followed by the embankment C_e 13%, both of which feature a notable variability across cases.

Design implications for LCOE can be appreciated in Fig. 9a that includes both original (Table 1) and redesigned cases (Table 6). For a 5% discount rate, the expected LCOE varies from 78 - 187 £/MWh. For redesigned cases excluding the outlier of R10 that has site-specific constraints, this range narrows to 71 - 136 £/MWh. We observe a quasi-linear logarithmic trend between LCOE and installed capacity, evidencing the scaling benefit associated with tidal range structures. Calculations of these results assumed a value of LCOE of around $r = 5\%$ [28]. However, the choice of discount rates varies among project developers, and it significantly influences LCOE estimations (Fig. 9b) given the project lifetime [22]. The Sustainable Development Commission's study [37] considers a plausible range of 3.5% to 15%. Nevertheless, a discount rate $> 12\%$ is regarded as excessively high while a value of 3.5% would unlikely attract investors [65].

Table 6: Predicted breakdown of cost components for a revised design of all schemes subject to a target capacity factor $C_F = 0.20$, efficiency $\eta_e = 0.40$, assumed turbine diameters $D = 7.35$ m, $A_s = 150$ m^2. The levelized cost of energy (LCOE) is computed with a discount rate $r = 5\%$. On operation, R1 and I1-I7 incorporate an adaptive two-way operation with fixed pump intervals following [19]. R2-R11 operate in an adaptive two-way mode, except for R4b and R7b, that feature an adaptive ebb-only strategy.

ID	Studies	C (GW)	N_t	N_s	CAPEX (£$_{2016}$ bn)	CAPEX/C (£$_{2016}$/W)	E_{yr} (TWh)	LCOE (£$_{2016}$/MWh)
	Realistic case studies							
R1	Swansea Bay Lagoon	0.20	10	5	0.73	3.65	0.38	116
R2	Stepping Stones Lagoon	0.47	19	10	2.04	4.34	0.90	136
R3	Cardiff Bay Lagoon	1.88	65	33	4.22	2.24	3.21	79
R4a	Welsh Grounds Lagoon	2.66	86	43	5.03	1.89	2.45	123
R4b	Welsh Grounds Lagoon	1.33	43	22	3.08	2.32	2.40	77
R5	Bridgwater Bay Lagoon	2.10	73	36	4.19	2.00	3.54	71
R6	West Somerset Lagoon	2.36	90	45	6.07	2.57	4.09	89
R7a	Cardiff-Weston Barrage	14.09	536	67*	25.36	1.80	12.39	123
R7b	Cardiff-Weston Barrage	7.05	268	134	15.43	2.19	11.68	79
R8	Outer Severn Barrage	20.26	973	122*	38.31	1.89	20.84	111
R9	Colwyn Bay Lagoon	2.16	132	66	6.12	2.83	3.53	104
R10	Mersey Barrage	0.71	36	18	3.97	5.59	1.27	187
R11	Morecambe Bay Barrage	2.33	20	60	5.93	2.49	3.89	92
	Idealised case studies							
I1	Swansea (SW)	0.78	37	18	2.32	2.97	1.37	102
I2	Cardiff (CA)	1.28	43	21	2.88	2.25	2.00	87
I3	Watchet (WA)	1.12	42	21	2.92	2.61	1.94	90
I4	Colwyn (CO)	0.57	33	17	1.95	3.42	1.03	114
I5	Liverpool (LI)	0.54	28	14	1.51	2.80	0.94	96
I6	Blackpool (BL)	0.66	35	18	2.07	3.14	1.18	105
I7	Solway (SO)	0.55	32	16	1.75	3.18	1.00	108

* Due to spatial constraints, the sluice number N_s was determined as 25% of the proposed predicted value.

4. Discussion

4.1. On the regional hydrodynamics modelling of tidal power plants

The coastal hydrodynamics define the resource available within the domain. Therefore, it is essential that the regional model used for the analysis represents the tidal range resource accurately at all sites where projects are considered. We opted to use a single domain to be consistent for several reasons. Firstly, any changes to the computational domain or mesh resolution strategy would require re-calibration, which would be a source of uncertainty [42]. The impacts of tidal range structures are non-intuitive and a baseline is conducive to the interpretation of comparative simulations [19]. An open research problem in studying tidal barriers regards the definition of the computational domain limits [66, 67], which must be sufficiently far to avoid notable interactions with the open sea boundaries [54, 53]. In this

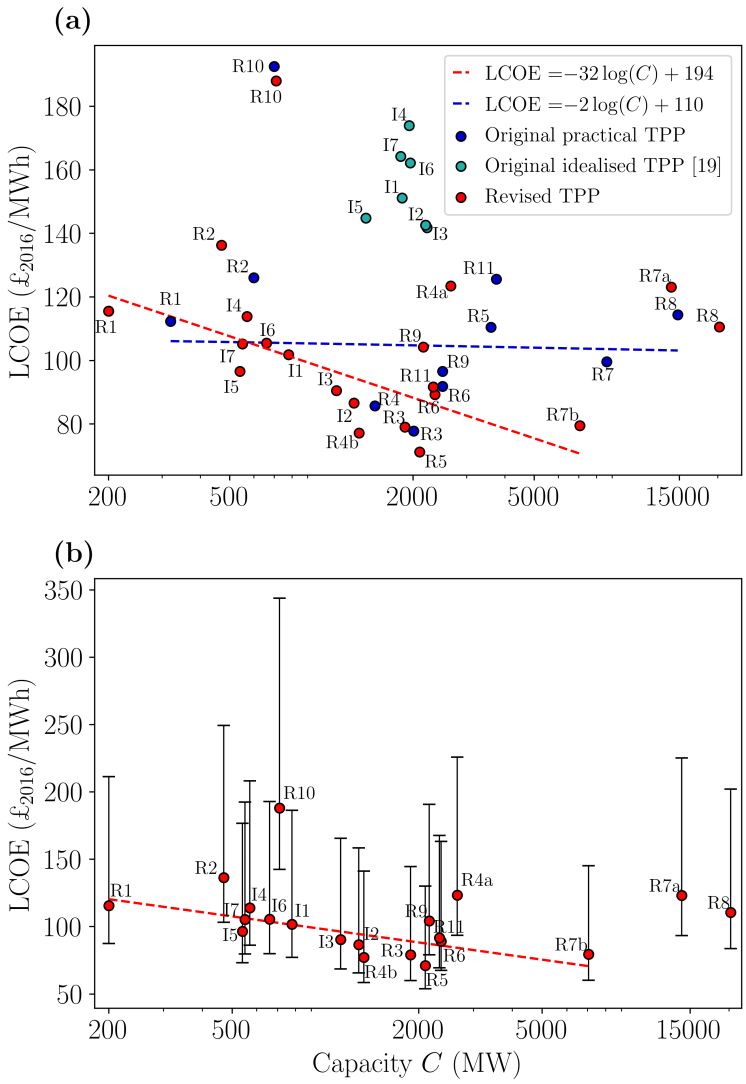

Figure 9: Levelised Cost of Electricity (LCOE) vs Capacity (C). (a) Inclusive of all tidal power plants for a discount rate $r = 5\%$. For illustration we include the best-fit linear logarithmic function between LCOE and C when considering the original (blue line) and revised designs (red line). (b) Constrained to revised designs, with error bars indicate the magnitude of uncertainty associated with varying discount rates from 3.5% to 15% as per [37].

case, we adopted the extends of a recent study that conducted a sensitivity with a cumulative capacity of 13.38 GW within the IS and the SEBC regions [19]. The open boundary position follows the recommended practice to extend to deep water conditions at the continental shelf [55], but not extending much further to require additional processes beyond regional modelling.

The open boundary forcing is imposed through spatially varying water elevation signals from TPXO9, allowing *Thetis* to define the appropriate boundary fluxes. While velocities could also be prescribed, it was considered over-constraining on model predictions. The

tidal energy flux entering the domain is therefore the result of the resistance introduced within the system through the calibration of the bed shear stress, which is known to be a source of uncertainty [68]. Different Manning's n fields show a challenge in capturing the dynamics using a uniform value approach, with spatial variations tested leading to the transfer of energy across tide constituents, as observed for n_2 in Fig. 5. The best performance was introduced by the additional resistance at Cardigan Bay and the localised scaling in IS and SEBC through n_3, which promotes a distribution of energy fluxes at SEBC and the IS (Fig. 5c) that is consistent with tide gauge observations without substantial interventions and non-physical values in the areas of interest where tidal power plants are located. For the analysis of tidal range structures this is substantial. For $n_1 = 0.026$ m$^{-1/3}$ s, we see significant underestimations in potential energy of $\approx$ –10% in the Severn Estuary, as opposed to overestimations of $\approx +10$ % in parts of the Irish Sea. The case of n_2 also leads to similar energy density distortions relative to observed gauge data (Fig. 6). Such an imbalance would translate to uneven feasibility metrics that could be non-negligible. For n_3 (Fig. 4) these deviations are more consistent, also capturing the equivalent variance in water elevation time series readings as in Fig. 6.

On other regional model set-up decisions we strike a balance between increasing complexity and capturing the key physics. A barotropic 2-D modelling approach is deemed sufficient for the conditions where the system is predominantly well-mixed [57], and primarily driven by hydraulic gradients on a horizontal plane as a result of the amplified tidal range. A depth-averaged approach enables the allocation of computational resource on sufficient resolution around the tidal range impoundment geometry while simulating runs over a lunar month to observe the hydrodynamic interactions with the resource. Indicatively, a lunar month-long simulation was performed within $\sim$ 5.5 hours on 12 CPU cores (Intel® Xeon® operating at 3.3 GHz).

4.2. On the evaluation of tidal power plants

The presence of tidal power plant barriers across sites demonstrates varying levels of hydrodynamic impact that is not necessarily proportional to the scale of the project as typically expected [5]. We see greatest impact associated with barrages that obstruct the entirety of the basin, disrupting the resonance and funneling phenomena behind tidal range amplifications. The case of the Mersey Barrage (R10) stands out as the barrage impact reduces the resource locally by a similar percentage as the much larger Severn Barrage (R7). On the other hand, the presence of designs of a greater capacity (e.g. the Welsh Grounds lagoon, R4) appear to have a negligible impact to the seaward resource (Table 4).

As with the variability in hydrodynamic impact, it is instructive to consider the geospatial variability on cost profile of tidal range projects. For example, dredging costs (see Fig. 7) can form a substantial cost component (reaching up to 15%). In a similar way, other components

show a substantial degree of variability (Fig. 8). Turbo-generators C_{t+g} and embankment C_e costs are the primary mechanical and civil costs respectively but they feature a notably wide range that can alter the order of significant costs. We consider this variability as one of the elements that add uncertainty in early feasibility studies of tidal range projects.

Even with such an uncertainty, comparisons between cost model predictions and reported values suggest an encouraging performance that enables us to draw conclusions when comparing sites. Indicatively, when considering the closest reported values (excluding the case of R5 as an outlier), the NRMSE error is on average at 12% which is an encouraging result considering several conflicting values reported previously in Table 5. A strength of this study is that it brings together multiple schemes across sites, of varying shape and scale and compares these consistently, based on a representative timeframe [48]. Cost analyses often focus on individual schemes [27] and include varying levels of operation modelling complexity and a diverse range of assumptions. Establishing a way forward through standardised analyses with guidance on modelling, optimisation and costing methods could contain performance uncertainty.

The benefits of such an approach that integrates hydrodynamics, operation optimisation, and economics becomes clear in Fig. 9. Tidal power plants that are uniformly designed for a higher C_F demonstrate a more attractive LCOE reduction rate with respect to installed capacity (as per the red logarithmic trend-line in Fig. 9). Several schemes were considered as outliers in these trends for specific reasons. The Mersey barrage (R10) [38] historically includes extensive lock components that exceed 40% of the CAPEX (the top outlier for C_l in Fig. 8). Two-way generation versions of the Welsh Grounds lagoon (R4a) and the Severn Barrage (R7a) perform poorly when modelled hydrodynamically. Therefore ebb-only alternatives (R4b, R7b) were considered instead that perform in a superior way. The performance issues of R7a and R4a are attributed to the impact of regulating flows through the hydraulic structures during operation, with *Thetis* predicting pressure surges upstream and downstream of the structure, which is a result of the geometry of the basin and the volume of water funneled through the structure. This has been demonstrated previously by several modelling studies [32, 34]. It is shown that the more conservative ebb-only designs for R4 and R7 designed based on half the resource $\beta = \frac{1}{2}$ in Eq. 9 suffer less hydrodynamic losses and are more efficient economically. An ebb-only Cardiff-Weston barrage (R7b) has a lower CAPEX and LCOE by 39% and 36 % respectively but only an energy yield sacrifice of 5.7%.

Contrary to the re-designed configurations, historic tidal power plant configurations reported in the literature (Table 5) follow a trend that is more insensitive to capacity (as per the blue logarithmic trend-line in Fig. 9b). We used the available data for these configurations, assessed impact and optimised operation as uniformly as possible, and yet we do not see

an apparent scaling benefit when considering original configurations of larger scale facilities. We attribute this to the lack of a standard approach to the design of tidal range structures that often treats hydro-environmental analyses separately to operation optimisation and cost feasibility assessments. If we consider the larger-scale schemes, design may still rely on 0-D models that incorporate corrections on the tidal range based on the far-field impact of the scheme. However, the same tools are incapable to capture features such as the surge effects emerging locally due to the hydraulic structure operation or the uneven water level within large basins considering intertidal areas. These bottlenecks compromise the application of standard 0-D models, which would need to be developed further to capture some of these non-linearities.

Shifting focus, it is interesting to contemplate the re-design performance of the idealised cases in Fig. 7. The objective function behind the original configuration in [19] underappreciated the cost of turbogenerators, opting to maximise energy yield. Though these schemes were designed consistently and having hydrodynamic impact and operation performance in mind, the resultant LCOE is distinctively higher than expected. The use of C_F as a target quantity contains the capacity in the re-designed cases and we see a reduction of both in the installed Capacity and the LCOE. This means that schemes could be perceived more feasible, given that capital costs are often cited as the bottleneck of the industry [5]. While these idealised cases were hypothetical, we see similar patterns for more high profile and extensively discussed schemes such as the Swansea Bay Lagoon (R1) [69]. Our predicted CAPEX for the original R1 would be at £1 bn and an LCOE of 113 £/MWh (Table 5). The re-designed version features a lesser capacity and the cost is contained to £0.73 bn and an LCOE of 116 £/MWh. This is a –27% reduction to CAPEX against a 3% increase to LCOE. Going forward, we see scope in containing capital costs through more conservative designs without compromising metrics that have previously challenged the project feasibility.

4.3. On assumptions, limitations and further developments

With a wide range of projects across spatial scales, assumptions have to be introduced to support a credible comparative basis. Nonetheless, the complexity of different projects means that different design and operation decisions will be implemented to further optimise individual schemes. By default, we assume that the standard operation strategy is going to be a two-way operation. It is expected that two-way operation features key environmental benefits over ebb-only operation including the broader distribution of power generation over the cycle, the preservation of mean water level (and by extension, groundwater level) in the impounded area, and the maintenance of certain flushing characteristics [11]. Separately, it is known that operating hydro-turbines in reverse as pumps has the potential to increase the net energy gains of tidal power plants [70]. A limited pumping capability was only considered in a single practical case (R1), and constrained to the idealised cases I1-7 [19]. We do not

use pumping extensively since (a) it favours smaller lagoons [20] and (b) the performance of tidal turbines operating as pumps is challenging to represent reliably. For that reason R2-11 exclude this, treating short-term pumped storage as an auxiliary function of the structure. In addition, in the redesign process a uniform turbine diameter D and sluice gate size A_s was assumed. For specific cases, further cost efficiency gains could be found on a balance of turbo-generator costs associated with greater D, which could impact on other cost components (e.g. dredging or powerhouse design). This is the case when comparing the original and redesigned versions of the Colwyn Bay Lagoon (R9), where the original yields a more attractive LCOE in Fig. 9a.

Providing fair cost estimates for design components is challenging given ever-evolving changes to their respective supply chains. We assume an uncertainty band of –20 to +20% around the typical value, recognising variance in capital and operating costs [71]. Nevertheless, this should be mitigated to an extend by the cost benchmarking exercise in Table 5 that suggests that the typical values used as inputs (Table 2) deliver sensible results. We then assumed a 5% discount rate, and acknowledge that interest/discount rates depend on the type of project developers [22]. Separately, economies of scale benefits associated with the larger schemes have not been included in the calculations. Grid integration costs of different power plants are not accounted for as these would be a function of existing infrastructure and future grid reinforcement plans as it adapts to a more decentralised and diverse energy system [72]. Other auxiliary benefits of tidal range projects are not evaluated. Examples involve flood risk mitigation along the coast of vulnerable communities (e.g. North Wales coastline), new transport links, the provision of regional redevelopment incentives, job creation opportunities etc. Moreover, omitting these benefits in the analysis is consistent with the approach of the 2017 UK Government review commissioned to study the potential of tidal range schemes [16].

For the representation and cost of turbines, sluice gates and related components, we relied on available information in the literature [49, 29, 37, 28]. These parameterisations could be replaced with updated and more specific quantities and formulations, that could reflect advances in turbo-machinery capabilities to unlock further cost-reduction pathways. An example is the development of variable speed turbine designs [73] that are more suited to low head hydropower applications that tidal range energy belongs. It is obvious that streamlining either the manufacture of turbine components or the costs of civil works associated with the impoundment would have a direct impact on the costs, and by extension the prospects of the tidal range energy industry.

Finally, operation optimisation in this work relied on a 0-D operation modelling approach that accounts for the far-field effects of tidal impoundments by using the modified tidal signals produced by *Thetis* [20]. This has proved effective for most designs in the study,

but substantial discrepancies arise between 0-D and 2-D predictions at high impact cases such as the Outer Severn Barrage (R8), the Cardiff-Weston Barrage (R7) and the Welsh Grounds lagoon (R4). These deviations relate to local hydrodynamic effects triggered by the substantial volume of water funnelled through the hydraulic structures relative to the basin width. Future corrections based on the basin geometry could be trialled to overcome this challenge, or otherwise the integration of PDE-constrained optimisation to include the momentum effects alongside the conservation of continuity.

5. Conclusion

This study operates on the hypothesis that an integrated design process that links hydrodynamic impact assessment, operation optimisation together with an economic analysis could have a transformative impact to the prospects of the tidal range energy sector. This study brings together advances on all these fronts to explore how design can be optimised for a technology that can support national, and global Net-Zero goals. In doing so, we showcase a design methodology for tidal power plants that is transferable and scalable with a potential to inform future tidal range energy developments.

We consider a combination of 18 hypothetical and historic tidal power plant along the coast, firstly based on reported configurations which are sequentially re-designed in a consistent manner to enable a comparative analysis. By re-designing schemes based on a target capacity factor of 0.2 and through exploring certain cases of alternative operation, a total of 38 different tidal power plants were modelled and assessed. We consider this the most comprehensive effort to date towards robustly assessing tidal power plants, considering hydrodynamic impacts, operation optimisation and cost breakdown.

The numerical experiments considering tidal power plants demonstrate that significant cost reduction pathways can be achieved through more conservative tidal power plant designs. We show that the same level of LCOE can be achieved with a lower capital (CAPEX) investment, in some cases in the order of –30%. We also see that the LCOE achieved over the project lifetime for typical redesigned cases ranges at 71-136 £/MWh based on a 5% interest rate. These cost projections are clearly much lower than other marine (wave & tidal) renewable options that currently exceed 200 £/MWh. We propose that an integrated hydrodynamic/operation and economic assessment framework, such as that developed here, could pave the way to meaningful optimisation of tidal power plant proposals and enable their deployment alongside other offshore renewable technologies.

Acknowledgements

K. Pappas acknowledges the support of Tidetec AS and the EPSRC WAMESS CDT (EP/S023801/1). A. Angeloudis acknowledges the support of the NERC Industrial Innova-

tion fellowship grant NE/R013209/2 and, together with N.Q. Chien, the support of the EC H2020 ILIAD DTO project under grant agreement 101037643.

References

[1] S. Neill, M. Hemmer, P. Robins, A. Griffiths, A. Furnish, A. Angeloudis, Tidal range resource of australia, Renewable Energy 170 (2021). doi:doi:10.1016/j.renene.2021.02.035.

[2] V. M. Barclay, S. P. Neill, A. Angeloudis, Tidal range resource of the Patagonian Shelf, Renewable Energy 209 (2023) 85–96. URL: https://www.sciencedirect.com/science/article/pii/S0960148123004433. doi:doi:10.1016/j.renene.2023.04.001.

[3] C. Mejia-Olivares, I. Haigh, A. Angeloudis, M. Lewis, S. Neill, Tidal range energy resource assessment of the Gulf of California, Mexico, Renewable Energy 155 (2020). doi:doi:10.1016/j.renene.2020.03.086.

[4] D. Pugh, P. Woodworth, Sea-level science: understanding tides, surges, tsunamis and mean sea-level changes, Cambridge University Press, 2014.

[5] S. P. Neill, A. Angeloudis, P. E. Robins, I. Walkington, S. L. Ward, I. Masters, M. J. Lewis, M. Piano, A. Avdis, M. D. Piggott, G. Aggidis, P. Evans, T. A. Adcock, A. Židonis, R. Ahmadian, R. Falconer, Tidal range energy resource and optimization – Past perspectives and future challenges, Renewable Energy 127 (2018) 763–778. URL: https://www.sciencedirect.com/science/article/pii/S0960148118305263. doi:doi:10.1016/j.renene.2018.05.007.

[6] T. M. Moreira, J. G. de Faria Jr, P. O. Vaz-de Melo, G. Medeiros-Ribeiro, Development and validation of an ai-driven model for the la rance tidal barrage: A generalisable case study, Applied Energy 332 (2023) 120506.

[7] R. Rtimi, A. Sottolichio, P. Tassi, C. Bertier, M. Le Brun, M. Vandenhove, L. Parquet, Three-dimensional hydrodynamic model of the rance estuary (france) influenced by the world's second largest tidal power plant, LHB 108 (2022) 1–8.

[8] A. Cornett, J. Cousineau, I. Nistor, Assessment of hydrodynamic impacts from tidal power lagoons in the Bay of Fundy, International Journal of Marine Energy 1 (2013) 33–54. URL: https://www.sciencedirect.com/science/article/pii/S2214166913000076. doi:https://doi.org/10.1016/j.ijome.2013.05.006.

[9] A. Nekrasov, D. Romanenkov, Impact of tidal power dams upon tides and environmental conditions in the sea of okhotsk, Continental Shelf Research 30 (2010) 538–552.

[10] Y. H. Bae, K. O. Kim, B. H. Choi, Lake sihwa tidal power plant project, Ocean Engineering 37 (2010) 454–463.

[11] A. Angeloudis, L. Mackie, M. D. Piggott, 8.06 - tidal range energy, in: T. M. Letcher (Ed.), Comprehensive Renewable Energy (Second Edition), second edition ed., Elsevier, Oxford, 2022, pp. 80–103. URL: https://www.sciencedirect.com/science/article/pii/B9780128197271000935. doi:doi:10.1016/B978-0-12-819727-1.00093-5.

[12] G. Todeschini, D. Coles, M. Lewis, I. Popov, A. Angeloudis, I. Fairley, F. Johnson, A. Williams, P. Robins, I. Masters, Medium-term variability of the UK's combined tidal energy resource for a net-zero carbon grid, Energy 238 (2022) 121990. URL: https://www.sciencedirect.com/science/article/pii/S0360544221022386. doi:doi:10.1016/j.energy.2021.121990.

[13] N. Yates, I. Walkington, R. Burrows, J. Wolf, Appraising the extractable tidal energy resource of the uk's western coastal waters, Philosophical Transactions of the Royal Society A: Mathematical, Physical and Engineering Sciences 371 (2013) 20120181.

[14] G. P. Hammond, C. I. Jones, R. Spevack, A technology assessment of the proposed Cardiff–Weston tidal barrage, UK, in: Proceedings of the Institution of Civil Engineers-Engineering Sustainability, volume 171, Thomas Telford Ltd, 2017, pp. 383–401. doi:https://doi.org/10.1680/jensu.16.00015.

[15] A. Angeloudis, R. A. Falconer, S. Bray, R. Ahmadian, Representation and operation of tidal energy impoundments in a coastal hydrodynamic model, Renewable Energy 99 (2016) 1103–1115. URL: https://www.sciencedirect.com/science/article/pii/S0960148116307042. doi:doi:10.1016/j.renene.2016.08.004.

[16] C. Hendry, The role of tidal lagoons. technical report, See https://hendryreview.com/, 2017.

[17] G. Clark, Oral statement to Parliament: Proposed Swansea Bay tidal lagoon, See https://www.gov.uk/government/speeches/proposed-swansea-bay-tidal-lagoon (accessed on 10 November 2023), 2018.

[18] R. Burrows, I. Walkington, N. Yates, T. Hedges, D. Chen, M. Li, J. Zhou, J. Wolf, R. Proctor, J. Holt, D. Prandle, Tapping the tidal power potential of the Eastern Irish Sea (2009). doi:10.13140/RG.2.2.35469.13285.

[19] L. Mackie, S. C. Kramer, M. D. Piggott, A. Angeloudis, Assessing impacts of tidal power lagoons of a consistent design, Ocean Engineering 240 (2021) 109879. URL: https://www.sciencedirect.com/science/article/pii/S0029801821012282. doi:doi:10.1016/j.oceaneng.2021.109879.

[20] A. Angeloudis, S. C. Kramer, A. Avdis, M. D. Piggott, Optimising tidal range power plant operation, Applied Energy 212 (2018) 680–690. URL: https://www.sciencedirect.com/science/article/pii/S0306261917317671. doi:doi:10.1016/j.apenergy.2017.12.052.

[21] F. Harcourt, A. Angeloudis, M. D. Piggott, Utilising the flexible generation potential of tidal range power plants to optimise economic value, Applied Energy 237 (2019) 873–884. URL: https://www.sciencedirect.com/science/article/pii/S0306261918319093. doi:doi:10.1016/j.apenergy.2018.12.091.

[22] D. R. Chalise, P. O'connor, S. Deneale, R. Uria-Martinez, S.-C. Kao, Lcoe uncertainty analysis for hydropower using monte carlo simulations, in: HydroVision International 2015 - Portland, Washington, United States of America, 2015, pp. 1–14. URL: https://dolraj.wordpress.ncsu.edu/files/2018/09/3-LCOE-Uncertainty-Analysis-for-Hydropower-using-Monte-Carlo-Simulations-20150801.pdf.

[23] A. Vazquez, G. Iglesias, LCOE (levelised cost of energy) mapping: A new geospatial tool for tidal stream energy, Energy 91 (2015) 192–201. URL: https://www.sciencedirect.com/science/article/pii/S0360544215010828. doi:doi:10.1016/j.energy.2015.08.012.

[24] Z. Goss, D. Coles, M. Piggott, Identifying economically viable tidal sites within the Alderney Race through optimization of levelized cost of energy, Philosophical Transactions of the Royal Society A 378 (2020) 20190500. URL: https://royalsocietypublishing.org/doi/10.1098/rsta.2019.0500. doi:doi:10.1098/rsta.2019.0500.

[25] D. Coles, A. Angeloudis, D. Greaves, G. Hastie, M. Lewis, L. Mackie, J. McNaughton, J. Miles, S. Neill, M. Piggott, et al., A review of the UK and British Channel Islands practical tidal stream energy resource, Proceedings of the Royal Society A 477 (2021) 20210469. URL: https://royalsocietypublishing.org/doi/10.1098/rspa.2021.0469. doi:doi:10.1098/rspa.2021.0469.

[26] J. A. Fay, M. A. Smachlo, Capital cost of small-scale tidal power plants, Journal

of Energy 7 (1983) 536–541. URL: https://doi.org/10.2514/3.62695. doi:doi:10.2514/3.62695. arXiv:https://doi.org/10.2514/3.62695.

[27] D. Vandercruyssen, D. Howard, G. Aggidis, A model of the costs for tidal range power generation schemes, Proceedings of the Institution of Civil Engineers - Energy 00058 (2022) 1–10. doi:doi:10.1680/jener.22.00058.

[28] D. Vandercruyssen, S. Baker, D. Howard, G. Aggidis, Tidal range generation: combining the Lancaster zero-dimension generation and cost models, Proceedings of the Institution of Civil Engineers - Energy (2023). URL: https://doi.org/10.1680/jener.22.00077. doi:doi:10.1680/jener.22.00077. arXiv:https://doi.org/10.1680/jener.22.00077.

[29] Black & Veatch, the University of Edinburgh, Tidal Modelling - Tidal Range Cost of Energy Model and Documentation, Technical Report, 2011. URL: https://ukerc.rl.ac.uk/cgi-bin/eti_query.pl?GoButton=DisplayLanding&etiID=699. doi:doi:10.5286/UKERC.EDC.000802.

[30] G. R. Timilsina, Are renewable energy technologies cost competitive for electricity generation?, Renewable Energy 180 (2021) 658–672. URL: https://www.sciencedirect.com/science/article/pii/S0960148121012568. doi:doi:10.1016/j.renene.2021.08.088.

[31] Parsons Brinckerhoff, Written evidence submitted by Parsons Brinckerhoff (SEV 07), See https://committees.parliament.uk/writtenevidence/43817/pdf/, 2012. URL: https://committees.parliament.uk/writtenevidence/43817/pdf/, (accessed: 16 August 2023).

[32] A. Angeloudis, R. A. Falconer, Sensitivity of tidal lagoon and barrage hydrodynamic impacts and energy outputs to operational characteristics, Renewable Energy 114 (2017) 337–351. URL: https://www.sciencedirect.com/science/article/pii/S0960148116307340. doi:doi:10.1016/j.renene.2016.08.033, wave and Tidal Resource Characterization.

[33] Department of Energy and Climate Change, Severn Tidal Power: Feasibility Study Conclusions and Summary Report, Ocean Engineering (2010).

[34] J. Xia, R. A. Falconer, B. Lin, Impact of different tidal renewable energy projects on the hydrodynamic processes in the Severn Estuary, UK, Ocean Modelling 32 (2010) 86–104. URL: https://www.sciencedirect.com/science/article/pii/S146350030900208X. doi:doi:10.1016/j.ocemod.2009.11.002.

[35] L. Mackie, D. Coles, M. Piggott, A. Angeloudis, The potential for tidal range energy systems to provide continuous power: A UK case study, Journal of Marine Science and Engineering 8 (2020). URL: https://www.mdpi.com/2077-1312/8/10/780. doi:doi:10.3390/jmse8100780.

[36] B. Guo, R. Ahmadian, R. A. Falconer, Refined hydro-environmental modelling for tidal energy generation: West Somerset Lagoon case study, Renewable Energy 179 (2021) 2104–2123. URL: https://www.sciencedirect.com/science/article/pii/S0960148121011940. doi:doi:10.1016/j.renene.2021.08.034.

[37] Black & Veatch, Research Report 3 - Severn Barrage Proposals, Technical Report, Sustainable Development Commission, 2007. URL: https://www.sd-commission.org.uk/data/files/publications/TidalPowerUK3-Severn_barrage_proposals.pdf.

[38] G. Aggidis, D. Benzon, Operational optimisation of a tidal barrage across the mersey estuary using 0-d modelling, Ocean Engineering 66 (2013) 69–81. URL: https://www.sciencedirect.com/science/article/pii/S0029801813001352. doi:doi:10.1016/j.oceaneng.2013.03.019.

[39] T. Kärnä, S. C. Kramer, L. Mitchell, D. A. Ham, M. D. Piggott, A. M. Baptista, Thetis coastal ocean model: discontinuous galerkin discretization for the three-dimensional hydrostatic equations, Geoscientific Model Development 11 (2018) 4359–4382.

[40] M. C. Clare, S. C. Kramer, C. J. Cotter, M. D. Piggott, Calibration, inversion and sensitivity analysis for hydro-morphodynamic models through the application of adjoint methods, Computers & Geosciences 163 (2022) 105104. URL: https://www.sciencedirect.com/science/article/pii/S0098300422000644. doi:doi:10.1016/j.cageo.2022.105104.

[41] A. K. Fragkou, C. Old, V. Venugopal, A. Angeloudis, Benchmarking a two-way coupled coastal wave–current hydrodynamics model, Ocean Modelling 183 (2023) 102193. URL: https://www.sciencedirect.com/science/article/pii/S1463500323000343. doi:doi:10.1016/j.ocemod.2023.102193.

[42] S. Warder, A. Angeloudis, M. Piggott, Sedimentological data-driven bottom friction parameter estimation in modelling Bristol Channel tidal dynamics, Ocean Dynamics (2021). URL: https://doi.org/10.1007/s10236-022-01507-x. doi:doi:10.1007/s10236-022-01507-x.

[43] F. Rathgeber, D. A. Ham, L. Mitchell, M. Lange, F. Luporini, A. T. T. Mcrae, G.-T. Bercea, G. R. Markall, P. H. J. Kelly, Firedrake: Automating the finite element

method by composing abstractions, ACM Trans. Math. Softw. 43 (2016) 24:1–24:27. URL: http://doi.acm.org/10.1145/2998441. doi:doi:10.1145/2998441.

[44] T. Kärnä, B. de Brye, O. Gourgue, J. Lambrechts, R. Comblen, V. Legat, E. Deleersnijder, A fully implicit wetting–drying method for DG-FEM shallow water models, with an application to the Scheldt Estuary, Computer Methods in Applied Mechanics and Engineering 200 (2011) 509–524. doi:doi:10.1016/j.cma.2010.07.001.

[45] A. Avdis, A. S. Candy, J. Hill, S. C. Kramer, M. D. Piggott, Efficient unstructured mesh generation for marine renewable energy applications, Renewable Energy 116 (2018) 842–856. URL: https://www.sciencedirect.com/science/article/pii/S0960148117309205. doi:doi:10.1016/j.renene.2017.09.058.

[46] S. Waters, G. Aggidis, Tidal range technologies and state of the art in review, Renewable and Sustainable Energy Reviews 59 (2016) 514–529. URL: https://www.sciencedirect.com/science/article/pii/S136403211501730X. doi:doi:10.1016/j.rser.2015.12.347.

[47] D. Prandle, Simple theory for designing tidal power schemes, Advances in Water Resources 7 (1984) 21–27. URL: https://www.sciencedirect.com/science/article/pii/0309170884900265. doi:doi:10.1016/0309-1708(84)90026-5.

[48] K. Pappas, L. Mackie, I. Zilakos, A. H. van der Weijde, A. Angeloudis, Sensitivity of tidal range assessments to harmonic constituents and analysis timeframe, Renewable Energy 205 (2023) 125–141. URL: https://www.sciencedirect.com/science/article/pii/S096014812300071X. doi:doi:10.1016/j.renene.2023.01.062.

[49] G. Aggidis, O. Feather, Tidal range turbines and generation on the Solway Firth, Renewable Energy 43 (2012) 9–17. URL: https://www.sciencedirect.com/science/article/pii/S0960148111006471. doi:doi:10.1016/j.renene.2011.11.045.

[50] L. Mackie, P. S. Evans, M. J. Harrold, O. Tim, M. D. Piggott, A. Angeloudis, Modelling an energetic tidal strait: investigating implications of common numerical configuration choices, Applied Ocean Research 108 (2021) 102494. URL: https://www.sciencedirect.com/science/article/pii/S0141118720310531. doi:doi:10.1016/j.apor.2020.102494.

[51] D. C. Rode, P. S. Fischbeck, The levelized cost of energy and regulatory uncertainty in plant lifetimes, Engineering Economist 66 (2021) 187–205. URL: https://doi.org/10.1080/0013791X.2021.1933283. doi:doi:10.1080/0013791X.2021.1933283.

[52] Department of Energy and Climate Change, Severn Tidal Power Feasibility Study - Phase 2, Technical Report, 2010.

[53] C. Gao, T. A. Adcock, On the tidal resonance of the Bristol Channel, International Journal of Offshore and Polar Engineering 27 (2017) 177–183. doi:doi:10.17736/ijope.2017.as19.

[54] C. Garrett, Tidal resonance in the Bay of Fundy and Gulf of Maine, Nature 238 (1972) 441–443. doi:doi:10.1038/238441a0.

[55] J. Zhou, S. Pan, R. A. Falconer, Optimization modelling of the impacts of a severn barrage for a two-way generation scheme using a continental shelf model, Renewable energy 72 (2014) 415–427. URL: https://www.sciencedirect.com/science/article/pii/S0960148114004340. doi:doi:10.1016/j.renene.2014.07.036.

[56] T. A. Adcock, S. Draper, G. T. Houlsby, A. G. Borthwick, SerhadloğluSena, The available power from tidal stream turbines in the pentland firth, Proceedings of the Royal Society A: Mathematical, Physical and Engineering Sciences 469 (2013) 20130072. doi:doi:10.1098/rspa.2013.0072.

[57] J. Wolf, I. A. Walkington, J. Holt, R. Burrows, Environmental impacts of tidal power schemes, in: Proceedings of the Institution of Civil Engineers-Maritime Engineering, volume 162, Thomas Telford Ltd, 2009, pp. 165–177. doi:10.1680/maen.2009.162.4.165.

[58] C. Binnie, Tidal energy from the Severn Estuary, UK, Proceedings of the Institution of Civil Engineers - Energy 169 (2016) 3–17. URL: https://doi.org/10.1680/jener.14.00025. doi:10.1680/jener.14.00025. arXiv:https://doi.org/10.1680/jener.14.00025.

[59] BBC News, Tidal lagoon: £1.3bn swansea bay project backed by review, See https://www.bbc.co.uk/news/uk-wales-38571240 (accessed on 20 September 2023), 2017. URL: https://www.bbc.co.uk/news/uk-wales-38571240.

[60] BBC News, £8bn cardiff tidal lagoon power deal 'agreed', See https://www.bbc.co.uk/news/uk-wales-41213528 (accessed on 20 September 2023), 2017. URL: https://www.bbc.co.uk/news/uk-wales-41213528.

[61] G. Jones, A. Jones, Severn Tidal Power Feasibility Study Assessment of the Regional Economic Impacts of Tidal Power Generation in the Severn Estuary Final Report, Technical Report, DTZ, 2009. URL: https:

//www.gov.wales/sites/default/files/statistics-and-research/2018-12/090126-tidal-power-generation-severn-estuary-en.pdf.

[62] Tidal Engineering and Environmental Engineering, Cost and revenue, See https://tidalengineering.co.uk/west-somerset-lagoon/cost-and-revenue/, 2019. URL: https://tidalengineering.co.uk/west-somerset-lagoon/cost-and-revenue/, (accessed on 12 September 2023).

[63] BBC News, Mersey estuary tidal power scheme 'will not go ahead', See https://www.bbc.co.uk/news/uk-england-merseyside-13875032 (accessed on 20 September 2023), 2011. URL: https://www.bbc.co.uk/news/uk-england-merseyside-13875032.

[64] Liverpool Business News, £6bn mersey tidal power scheme hangs in balance, See https://lbndaily.co.uk/6bn-mersey-tidal-power-scheme-hangs-in-balance (accessed on 20 September 2023), 2022. URL: https://lbndaily.co.uk/6bn-mersey-tidal-power-scheme-hangs-in-balance/.

[65] IPA Energy and Water Consulting, Severn Barrage Costing Exercise, Technical Report, The Renewable Energy Forum Ltd, 2008. URL: https://www.ref.org.uk/attachments/article/144/ipa.for.ref.severn.barrage.study.1.pdf.

[66] C. Garrett, D. Greenberg, Predicting changes in tidal regime: the open boundary problem, Journal of Physical Oceanography 7 (1977) 171–181. doi:doi:10.1175/1520-0485(1977)007<0171:PCITRT>2.0.CO;2.

[67] D. Prandle, Modelling of tidal barrier schemes: an analysis of the open-boundary problem by reference to ac circuit theory, Estuarine and Coastal Marine Science 11 (1980) 53–71. URL: https://www.sciencedirect.com/science/article/pii/S0302352480800296. doi:doi:10.1016/S0302-3524(80)80029-6.

[68] M. J. Kreitmair, S. Draper, A. G. L. Borthwick, T. S. van den Bremer, The effect of uncertain bottom friction on estimates of tidal current power, Royal Society Open Science 6 (2019) 180941. URL: https://royalsocietypublishing.org/doi/abs/10.1098/rsos.180941. doi:10.1098/rsos.180941. arXiv:https://royalsocietypublishing.org/doi/pdf/10.1098/rsos.180941.

[69] S. Waters, G. Aggidis, A world first: Swansea bay tidal lagoon in review, Renewable and Sustainable Energy Reviews 56 (2016) 916–921. URL: https://www.sciencedirect.com/science/article/pii/S1364032115013945. doi:doi:10.1016/j.rser.2015.12.011.

[70] N. Yates, I. Walkington, R. Burrows, J. Wolf, The energy gains realisable through pumping for tidal range energy schemes, Renewable energy 58 (2013) 79–84. URL: https://www.sciencedirect.com/science/article/pii/S0960148113000773. doi:doi:10.1016/j.renene.2013.01.039.

[71] Poyry Management Consulting, Levelised cost of power from tidal lagoons. technical report, See https://tinyurl.com/5n7a4z6z, 2014.

[72] D. Pudjianto, C. Frost, D. Coles, A. Angeloudis, G. Smart, G. Strbac, Uk studies on the wider energy system benefits of tidal stream, Energy Advances (2023). doi:doi:10.1039/D2YA00251E.

[73] J. Fraile-Ardanuy, J. R. Wilhelmi, J. J. Fraile-Mora, J. I. Pérez, Variable-speed hydro generation: operational aspects and control, IEEE Transactions on energy conversion 21 (2006) 569–574.